Effect of red and near-infrared wavelengths on low-level laser (light) therapy-induced healing of partial-thickness dermal abrasion in mice

Citation: Gupta, Asheesh, Tianhong Dai, and Michael R. Hamblin. "Effect of Red and near-Infrared Wavelengths on Low-Level Laser (Light) Therapy-Induced Healing of Partial-Thickness Dermal Abrasion in Mice." Lasers in Medical Science 29.1 (2014): 257–265.

As Published: http://dx.doi.org/10.1007/s10103-013-1319-0

Publisher: Springer London

Persistent URL: http://hdl.handle.net/1721.1/104348

Version: Author's final manuscript: final author's manuscript post peer review, without publisher's formatting or copy editing

Lasers Med Sci (2014) 29:257–265
DOI 10.1007/s10103-013-1319-0

ORIGINAL ARTICLE

Effect of red and near-infrared wavelengths on low-level laser (light) therapy-induced healing of partial-thickness dermal abrasion in mice

Asheesh Gupta · Tianhong Dai · Michael R. Hamblin

Received: 19 June 2012 / Accepted: 10 April 2013 / Published online: 26 April 2013

Abstract Low-level laser (light) therapy (LLLT) promotes wound healing, reduces pain and inflammation, and prevents tissue death. Studies have explored the effects of various radiant exposures on the effect of LLLT; however, studies of wavelength dependency in in vivo models are less common. In the present study, the healing effects of LLLT mediated by different wavelengths of light in the red and near-infrared (NIR) wavelength regions (635, 730, 810, and 980 nm) delivered at constant fluence (4 J/cm^2) and fluence rate (10 mW/cm^2) were evaluated in a mouse model of partial-thickness dermal abrasion. Wavelengths of 635 and 810 nm were found to be effective in promoting the healing of dermal abrasions. However, treatment using 730- and 980-nm wavelengths showed no sign of stimulated healing. Healing was maximally augmented in mice treated with an 810-nm wavelength, as evidenced by significant wound area reduction ($p<0.05$), enhanced collagen accumulation, and complete re-epithelialization as compared to other wavelengths and non-illuminated controls. Significant acceleration of re-epithelialization and cellular proliferation revealed by immunofluorescence staining for cytokeratin-14 and proliferating cell nuclear antigen ($p<0.05$) was evident in the 810-nm wavelength compared with other groups. Photobiomodulation mediated by red (635 nm) and NIR (810 nm) light suggests that the biological response of the wound tissue depends on the wavelength employed. The effectiveness of 810-nm wavelength agrees with previous publications and, together with the partial effectiveness of 635 nm and the ineffectiveness of 730 and 980 nm wavelengths, can be explained by the absorption spectrum of cytochrome c oxidase, the candidate mitochondrial chromophore in LLLT.

Keywords Cytokeratin-14 · Low-level laser (light) therapy · Near-infrared · Partial-thickness abrasion · Photobiomodulation · Proliferating cell nuclear antigen (PCNA)

A. Gupta · T. Dai · M. R. Hamblin (✉)
BAR414, Wellman Center for Photomedicine, Massachusetts General Hospital, 40 Blossom Street, Boston, MA 02114, USA
e-mail: hamblin@helix.mgh.harvard.edu

A. Gupta · T. Dai · M. R. Hamblin
Department of Dermatology, Harvard Medical School, Boston, MA 02115, USA

A. Gupta
Defence Institute of Physiology & Allied Sciences, Delhi 110 054, India

M. R. Hamblin
Harvard-MIT Division of Health Sciences and Technology, Cambridge, MA 02139, USA

Introduction

The use of laser or other light sources at non-thermal irradiances for healing and relief of pain and inflammation (among other medical applications) is known as low-level laser (or light) therapy (LLLT), phototherapy, or photobiomodulation. In the past few decades, a large number of reports demonstrating the positive effects of LLLT in various in vitro [1–7], in vivo [5, 8–12], and clinical studies [13–16] have been published. LLLT has emerged in recent years as a noninvasive physical modality for various musculoskeletal, neurological, and cutaneous disorders [17]. LLLT involves exposing cells or tissues to low-levels of red and near-infrared (NIR) light and is referred to as "low-level" because of the use of light at energy or power densities that are low compared to other forms of laser therapy that are used for ablation, cutting, and thermally coagulating tissue.

The mechanism associated with photobiostimulation by LLLT is not yet fully understood. It appears that LLLT has a wide range of effects at the molecular, cellular, and tissular levels. The basic biological mechanism behind the effects of LLLT is thought to be through the absorption of red and NIR light by chromophores, in particular cytochrome c oxidase (CCO), which is unit IV in the respiratory chain located within the mitochondria [18], and perhaps also chromophores in the plasma membrane of cells; thereafter, a cascade of events occur in the mitochondria, leading to the biostimulation of various processes [19]. The absorption spectra obtained for CCO in different oxidation states were recorded and found to be very similar to the action spectra for biological responses to LLLT [18]. It is assumed that this absorption of light energy may cause photodissociation of the inhibitory nitric oxide from CCO [20], leading to the enhancement of enzyme activity [21], increased electron transport [22], oxygen consumption, mitochondrial respiration, and ATP production [23]. In turn, LLLT, by altering the mitochondrial or cellular redox state, can induce the activation of numerous intracellular signaling pathways and alter the affinity of transcription factors concerned with cellular migration, proliferation, survival, tissue repair, and regeneration [18].

Although LLLT is now used to treat a wide variety of ailments, it still remains somewhat controversial as a therapy for two principal reasons: firstly, there remain uncertainties about the fundamental molecular and cellular mechanisms responsible for transducing signals from the photons incident on the cells to the biological effects that take place in the irradiated tissue. Secondly, a large number of dosimetry parameters are mainly categorized into two ways, i.e., the irradiation or the "medicine" (wavelength, irradiance or power density, pulse structure, coherence, polarization) and the delivered fluence or "dose" (energy, fluence, irradiation time, repetition regimen). A less than optimal choice of parameters can result in the reduced effectiveness of the treatment or even a negative therapeutic outcome [17]. As a result, many of the published studies on LLLT include negative results simply because of an inappropriate choice of light source and dosage [24]. It is important to consider that there is an optimal dose of light for any particular application, and doses higher or lower than this optimal value may have no therapeutic effect. In fact, one important point that has been demonstrated by multiple studies is the concept of a biphasic dose response depicted by LLLT [17]. Laser radiation or non-coherent light has a wavelength- and radiant exposure-dependent capability to alter cellular behavior in the absence of significant heating [25]. Phototherapy includes wavelengths of between 500 and 1,100 nm and typically involves the delivery of 1–4 J/cm^2 to treatment sites. There is a considerable debate in the literature about the differences between the cellular effects of monochromatic laser light and polychromatic light from non-laser light sources [16, 26]. In this context, earlier, our group demonstrated that LLLT stimulated healing of excision-type dermal wounds in mice and reported no difference between non-coherent 635±15-nm light and coherent 632.8-nm laser [8] irradiations performed using the same spot size and the same fluence (2 J/cm^2). While there are various studies exploring the effects of different power and energy densities on the outcome of treatment, however, studies of wavelength dependency, especially in in vivo models, are less widespread. In view of the wide variety of different light sources available to perform LLLT, it is important to define all parameters exactly so that studies can be compared with each other.

Since light has a wavelength-dependent capability to alter cellular behavior, hence, in the present study, the healing effects of LLLT mediated by different wavelengths of light in the red and NIR wavelength regions (635, 730, 810, and 980 nm) delivered at constant fluence (4 J/cm^2) and fluence rate (10 mW/cm^2) were evaluated in a mouse model of partial-thickness dermal abrasion. This study aimed to identify the light wavelength that would augment the healing process by improving wound contraction, cellular proliferation, collagen deposition, and re-epithelialization in partial-thickness dermal abrasions.

In this study, we used a mouse model of a partial-thickness dermal abrasion to mimic the dermal scrape in humans (skin trauma including sports, road accidents, and combat situations). Dermal abrasions are wounds that rub or tear off the upper layer of the skin comprising the epidermis and partially damaged dermis up to the subcutaneous layer. Human wound healing is governed by re-epithelialization, not by contraction, which is commonly observed in excision-type wound healing in animals. Animals possess a subcutaneous panniculus carnosus muscle which contributes to the repair via contraction and collagen formation. However, this structure is absent in humans. The present partial-thickness dermal abrasion mouse model was used to evaluate the effect of LLLT in a wound healing model where re-epithelialization is the dominant mode of healing rather than wound contraction and which also represents high clinical relevance. Furthermore, in this study, the re-epithelialization and cellular proliferation in the LLLT-induced partial-thickness dermal abrasion were monitored using specific molecular markers, viz., cytokeratin-14 and proliferating cell nuclear antigen (PCNA), respectively.

Methods

Animals

The experiments were approved by the Subcommittee on Research Animal Care of Massachusetts General Hospital

(IACUC) and were in accordance with NIH guidelines. Adult male BALB/c mice (Charles River Laboratories, Wilmington, MA), 7–8 weeks old and weighing 18–20 g, were used in this study. The animals were housed one per cage (to prevent cage mate attacks on wounds) and had access to food and water ad libitum. The mice were maintained on a 12–h light/dark cycle under a room temperature of 21 °C.

Mouse model of partial-thickness dermal abrasion

The animals were anesthetized by an intraperitoneal (i.p.) injection of a ketamine–xylazine cocktail (90 mg/kg ketamine and 10 mg/kg xylazine) before the wounding procedure and during follow-up treatment. The dorsal surface of the mouse was shaved using an electric fur clipper and the underlying skin was cleaned with sterile 70 % isopropanol. Mouse skin was then scraped with no. 15 sterile scalpel blades (Feather Safety Razor Co. Ltd., Osaka, Japan) until a reddened area appeared. This procedure resulted in partial-thickness skin abrasions with removed epidermis and partially damaged dermis up to the subcutaneous layer with some oozing of a small amount of blood, the surface becoming dark red. Each wound measured approximately 1.2×1.2 cm. The wound was left uncovered during the whole period of experiments. Previous histological analysis revealed that the epidermis and partial dermis up to the subcutaneous layer were completely injured.

Experimental design

Four light sources were used in this study for irradiation. A non-coherent light source with interchangeable 30-nm band pass filters (LumaCare, London, UK) was used to deliver 635±15-nm light, a 730-nm diode laser (Pharmacyclics Cambridge, UK), an 810-nm diode laser (Acculaser, Photothera Inc., Carlsbad, CA), and a 980-nm diode laser (V-Raser, HoyaConBio, Fremont, CA). All the lasers were coupled into a fiber-optic that was arranged to deliver a light spot centered on the dorsal surface of the mouse with the dermal abrasion. The fluence rates were measured with a power meter (PM 100D with Standard head, Thorlabs Gmbh, Dachau, Germany) and adjusted to be 10 mW/cm^2. Table 1 depicts the irradiation parameters for partial-thickness dermal abrasion in mice.

A total of 30 mice were randomly divided into five groups of six mice per group, comprising four experimental and one non-illuminated control group. Experimental groups of mice received single illumination with 635-, 730-, 810-, or 980-nm light irradiation, respectively (at the constant fluence of 4 J/cm^2) 30 min post-injury. The irradiations were performed in the same manner with the different probes. The spot of the light beam had an area of 2.25 cm^2 that covered the entire dermal abrasion including the surrounding normal tissue to stimulate unwounded dermal cells (keratinocytes and endothelial cells) to migrate into the wounded area. Non-illuminated control mice with dermal abrasions were kept anesthetized for the same length of time as the illuminated mice. Control abrasions received no light and were left to heal spontaneously.

Irradiation was delivered once daily for seven consecutive days. The wounds were observed daily and wound images were acquired on 0, 1, 2, 4, and 8 days post-injury using a charge-coupled device camera (Olympus PEN E-PL1). Mice were killed by CO_2 inhalation on the eighth day post-injury and skin samples were carefully collected to include the adjacent healthy tissue and all the healed tissue to perform histopathological and immunohistochemistry analysis.

Wound area measurement

Wound surface area was monitored by capturing the video images of each partial-thickness abrasion together with a ruler (in millimeters) using the Olympus digital camera and downloaded to a computer. The first image of each abrasion wound from the different groups was obtained on the day of injury (day 0). Subsequent images were captured on the first, second, fourth, and the eighth day post-injury. Wound area analysis was performed using Fiji (ImageJ) software; values were expressed in square millimeters. Repeated measurements were accurate to within 2 %.

Table 1 Irradiation parameters for partial-thickness dermal abrasion in mice

Wavelength (nm)	635±15	730	810	980
Mode	CW lamp	CW laser	CW laser	CW laser
Fluence rate (mW/cm^2)	10	10	10	10
Fluence (J/cm^2)	4	4	4	4
Power (mW)	22.5	22.5	22.5	22.5
Energy (J)	9	9	9	9
Time of irradiation/day (min)	6.6	6.6	6.6	6.6
Spot size on mouse (cm^2)[a]	2.25	2.25	2.25	2.25
No. of animals (controls, n=6)	6	6	6	6

CW continuous wave

[a]Spot size was defined by the area of the square window in the aluminum foil (1.5×1.5 cm) used to cover the mouse body. Each wound measured approximately 1.2×1.2 cm

Histological studies

The regenerated skin tissues were preserved in 10 % phosphate–buffered formalin (Fisher Scientific, USA) for 18–24 h, processed, and then embedded in paraffin. Serial tissue sections of 4-μm thickness were prepared, stained with hematoxylin and eosin (H&E), and observed for histological changes under a light microscope (Axiophot, Carl Zeiss Microscope, Thornwood, NY). Gomori Trichrome staining (Leica Microsystem, USA) for collagen was also performed on paraffin sections, followed by photomicrography.

Immunohistochemistry for PCNA and cytokeratin-14

PCNA is a 36-kDa polypeptide and is known to be strongly expressed in the nuclear region of cells where DNA synthesis is occurring. Cytokeratin-14 is a 50-kDa polypeptide found in the basal cells of squamous epithelia, glandular epithelia, myoepithelium, and mesothelial cells and also found in keratinocytes surrounding the club hair during the hair production resting phase (telogen). Epithelialization originated from adnexal structures in which epithelial islets showed positive staining for cytokeratin-14 and PCNA. In the present study, changes in the mitotic rate (cell proliferation) and re-epithelialization following dermal abrasion in mice treated with LLLT were studied immunohistochemically (IHC) using PCNA and cytokeratin-14 primary antibodies, respectively.

Briefly, sections were deparaffinized in Citrisolv solution (Fisher Scientific) and rehydrated with descending ethanol series. After antigen retrieval (Dako North America Inc., CA), tissue sections were permeabilized with Triton-X 100 (0.1 %) followed by blocking with 10 % goat serum in PBS at 37 °C for 30 min. After that, the tissue sections were incubated with the primary antibody against rabbit polyclonal to PCNA (1:500; Abcam, Boston, MA) at 4 °C overnight and the fluorescence-labeled secondary antibody (Alexa Fluor-680 goat anti-rabbit IgG, 1:500; Invitrogen, Carlsbad, CA) in the dark for 1 h at room temperature, washed with PBS, and coverslipped with mounting media including diamidino–2–phenylindole (DAPI; SlowFade Gold anti-fade reagent, Invitrogen). Negative controls were treated with PBS instead of the primary antibody.

For cytokeratin-14 IHC staining, a primary antibody against mouse monoclonal to cytokeratin-14 (Abcam) was used. Tissue sections were processed in a similar way as PCNA until the permeabilization step. After that, a further procedure was performed using Vector Mouse-on-Mouse (M.O.M.) Immunodetection Kit (Vector Laboratories Inc., Burlingame, CA) following the instructions supplied by the manufacturer. Briefly, tissue sections were incubated for 30 min at room temperature with anti–cytokeratin-14 (1:200) followed by incubation with M.O.M. biotinylated anti–mouse IgG reagent (second antibody) for 10 min at room temperature. Then, the tissue sections were incubated in the dark for 5 min at room temperature with Fluorescein Avidin DCS (Vector Laboratories). Between the incubations, the tissue sections were extensively washed in PBS. The sections were then mounted with coverslips using a mounting medium with DAPI.

Fluorescent images were obtained using an Olympus Fluoview FV1000-MPE multiphoton confocal microscope (Olympus Corporation, Tokyo, Japan) to image the LLLT-treated tissue sections. The microscope used excitation wavelengths of 488 nm for fluorescein, 647 nm for Alexa Fluor-680, and 405 nm for DAPI-associated fluorescence. DAPI was used as the nuclear counter stain. The emission signals were observed using a set of band-pass filters for DAPI (425–475 nm), fluorescein (505–556 nm), and Alexa Fluor-680 (660–760 nm) and the images acquired using the Olympus Fluoview FV10-ASW software, version 3.0a (Olympus Corporation). Furthermore, images were merged and signals of the integrated fluorescence intensity were quantitatively analyzed at ×60 magnification using Fiji (ImageJ) software. In the confocal fluorescence micrographs, fluorescence from PCNA, cytokeratin-14, and DAPI was pseudo-colored red, green, and blue, respectively, to make superimposition more visible.

Statistical analysis

Data are presented as the mean±SE. Differences in the wound surface area and integrated immunofluorescence intensity (PCNA and cytokeratin-14) between the non-illuminated control and different wavelengths of light-treated groups were compared for statistical significance using one-way ANOVA followed by Dunnett's post hoc test using Graph Pad Prism 5.0 (Graph Pad Software Inc., La Jolla, CA). A p value<0.05 was considered statistically significant.

Results

Wound area evaluation after LLLT

In the present study, we compared four different wavelength ranges of red and NIR lights centered at 635, 730, 810, and 980 nm delivered at a constant fluence (4 J/cm^2) and fluence rate (10 mW/cm^2) to study dermal wound healing response variation with wavelength. Table 2 depicts the effect of light treatment with different wavelengths on the wound area. Illuminated wounds treated with different wavelengths exhibited wound contraction from day 1 until observation of day 8 post-injury. However, non-illuminated control wounds initially expanded on day 1 post-injury, and at day 2, control wounds were the same size as the original size on day 0. From day 4 onwards, control wound exhibited

Table 2 Effect of the wavelength of light on wound surface area (in square millimeters) of partial-thickness dermal abrasion in mice

Post-wounding day	Control	Wavelength of light			
		635 nm	730 nm	810 nm	980 nm
Day 0	147.0±2.1	143.8±1.2	148.2±1.9	146.7±1.7	145.8±1.4
Day 1	169.0±1.6 (−15)	117.6±1.6*(18)	134.6±3.4* (9)	112.9±3.2* (23)	126.5±8.0*(13)
Day 2	146.9±10.5	104.1±2.1* (28)	119.2±2.7*(20)	91.2±3.5*(38)	114.3±8.4*(22)
Day 4	91. 0±10.4 (38)	95.3±1.1 (34)	105.7±3.0 (29)	67.2±4.1*(54)	101.9±7.0 (30)
Day 8	59.2±6.4 (60)	52.3±1.5 (64)	48.0±3.3 (68)	41.9±3.6* (71)	60.5±4.1 (59)

Values are the mean±SE (n=6 per group). Numbers in parenthesis indicate the percentage of wound contraction. Wounds received no illumination (control) and single exposure daily to different wavelengths (635-, 730-, 810-, or 980-nm light) delivered at constant fluence (4 J/cm^2) and fluence rate (10 mW/cm^2)

*p<0.05 (compared with non-illuminated control)

a gradual reduction in wound area. Days 4 and 8 post-injury revealed that mice treated with 810 nm had a significant reduction in wound area compared with the non-illuminated control mice (p<0.05). However, no significant differences were detected in other groups treated with 635-, 730-, and 980-nm light at 4 and 8 days post-injury (Table 2).

Morphological changes after LLLT

Multiple cross-sections of H&E-stained sections of light-treated and untreated dermal wound tissues of mice were examined for epithelial regeneration, formation of granulation tissue, and fibrogenesis. The non-illuminated control wounds showed a denuded epithelium, and the wound itself showed a number of inflammatory cells, such as neutrophils and lymphocytes and scattered fibroblasts at day 8 post-injury (Fig. 1). In contrast, histopathological examinations indicated that 635 and 810 nm were effective in promoting repair of partial-thickness dermal abrasion in mice. The most pronounced stimulation of wound healing as evidenced by enhanced organization and initiation of fibrogenesis, neovascularization, and complete re-epithelialization was observed in 810 nm compared to the 635-nm treated wounds. However, 730- and 980-nm treated wounds showed no sign of healing. Moreover, 980-nm treatment revealed edema, denuded epithelium, and persisting inflammatory infiltrate in the wound bed (Fig. 1).

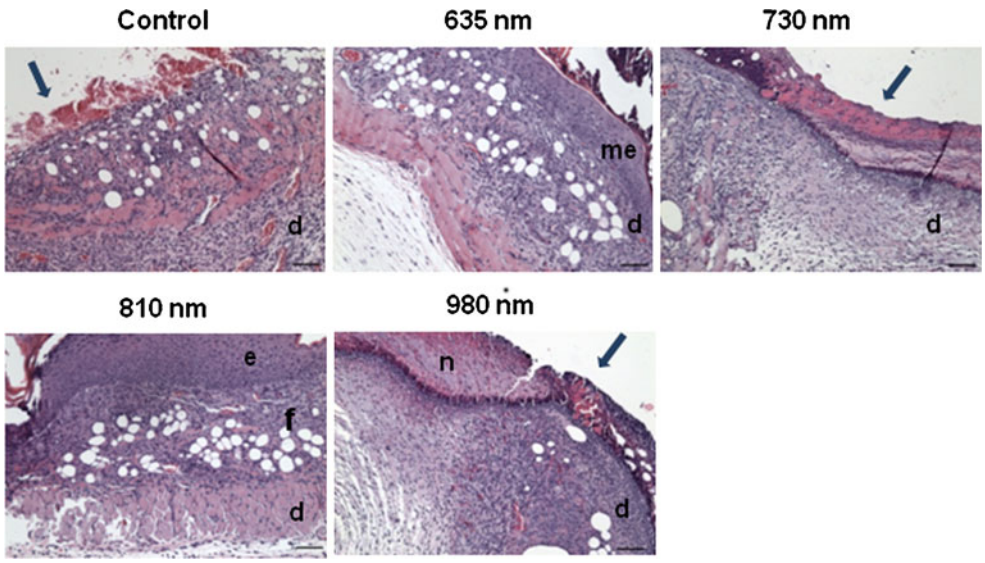

Fig. 1 Histopathological changes on day 8 post-injury in partial-thickness dermal abrasion in mice. H&E-stained sections of non-illuminated control show denuded epidermis and infiltration of inflammatory cells in the wound bed. On the other hand, 635- and 810-nm light treatment resulted in enhanced fibrosis, collagen accumulation, neovascularization, and re-epithelialization. Healing effect was more pronounced in the 810-nm compared with the 635-nm light. Light treatment of 810 nm showed a wound surface with a well-organized thick epithelium. However, 730- and 980-nm light-treated wounds showed no sign of healing. Light treatment of 980 nm showed edema and denuded epidermis with a marked infiltration of inflammatory cells in the wound bad. *Scale bar*, 100 μm (*bottom panels*). *d* dermis, *e* epidermis, *f* fibrosis, *me* migrating tongue of the epidermis, *n* necrotic tissue. *Arrows* show denuded epithelialization in the case of non-illuminated control and light (730 and 980 nm) treated wounds

The extent of collagen deposition in the wound granulation tissue was examined by trichrome staining (Fig. 3). Treatment of 810 nm resulted in enhanced collagen accumulation in the wounds compared with the other light-treated groups and non-illuminated control. Non-illuminated control wounds had a loose reticular arrangement of collagen, whereas collagen was compact and well aligned in the 810-nm treated wounds (Fig. 2).

IHC localization of PCNA and cytokeratin-14 after LLLT

Figures 3 and 4 show IHC staining for PCNA and cytokeratin-14 after treatment with different wavelengths of light at day 8 post-injury. Quantitative analysis of immunofluorescence intensity revealed a significant increase in PCNA located in the epidermis–dermis (3- to 14-fold) and also in epidermal cytokeratin-14 expression (6- to 20-folds) in 810-nm treated wounds compared with the non-illuminated control and other light-treated wounds ($p<0.05$). However, 635-nm treatment showed a trend for increasing PCNA and cytokeratin-14 expressions compared with the controls that did not reach significance. There was no difference in the expression of PCNA and cytokeratin-14 in 730- and 980-nm light-treated wounds compared with the control. Negative control demonstrated no staining (not shown).

Discussion

A light beam applied to live tissue will have different effects on the tissue components dependent upon the wavelength of the radiation and the tissue component's susceptibility to different wavelengths. The aim of this study was to evaluate the effects of light wavelength by delivering at constant fluence (4 J/cm^2) and fluence rate (10 mW/cm^2) four different wavelengths (635, 730, 810, and 980 nm) of light in a mouse model of partial-thickness dermal abrasion. The results of the present study indicated that light-irradiated wounds resulted in a significant reduction in wound area. Interestingly, a marked difference between the illuminated and non-illuminated control wounds was observed at day 1 post-injury. Control wounds showed an expansion on day 1 in the wound area, being almost 15 % bigger than it was immediately after wounding. However, the illuminated wounds treated with different wavelengths decreased in wound area after light delivery on days 1 and 2 post-injury. However, later days post-injury (days 4 and 8) demonstrated no significant differences in wound area contraction of the control compared with the light-treated groups (635, 730, and 980 nm). Remarkably, the wound area was found significantly reduced in 810-nm light-treated wounds at days 4 and 8 post-injury compared with the control. In this study, we demonstrated that both red (635 nm) and NIR (810 nm) lights can significantly enhance the healing of partial-thickness dermal abrasions. Similarly, other studies have also reported that He–Ne laser (632.8 nm) and other wavelength (660–670 nm) irradiations at a fluence of 1–6 J/cm^2 stimulated healing in normal and impaired wounds (burns and diabetic) by re-epithelialization and granulation tissue formation [8, 9, 11, 27, 28].

Interestingly, the results of the present study indicate that NIR lasers at 730 or 980 nm did not produce the same beneficial positive effects on dermal abrasion. The most pronounced stimulation of healing in dermal abrasion was observed in 810-nm treatment, as evidenced by significant wound area contraction and enhanced collagen accumulation, neovascularization, and complete re-epithelialization compared with the 635-nm-treated and non-illuminated control. A significant enhancement of re-epithelialization and cellular proliferation revealed by positive immunofluorescence staining for cytokeratin-14 and PCNA across the

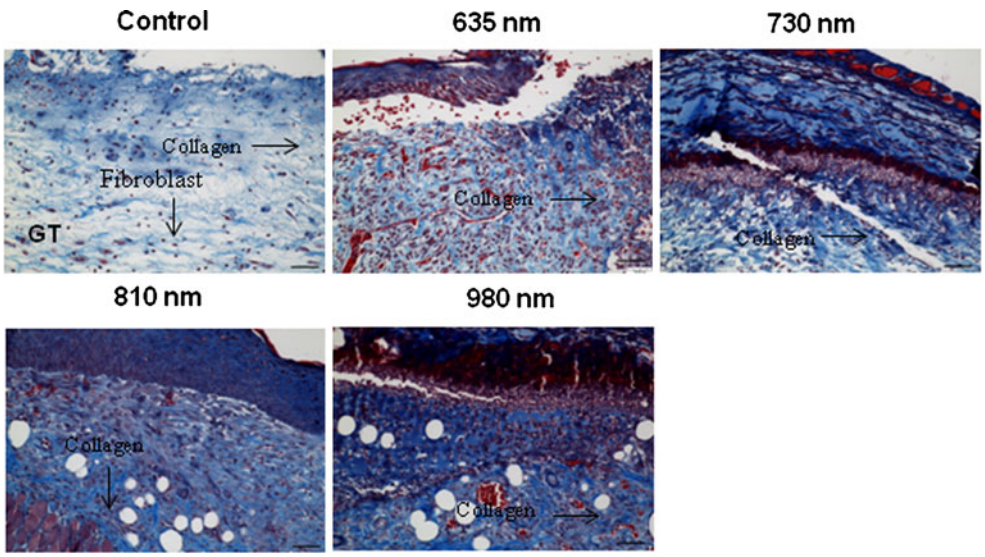

Fig. 2 Trichrome staining shows collagen on day 8 post-injury in partial-thickness dermal abrasions in mice. Sections of non-illuminated control and other light (635, 730, and 980 nm) treated groups showed less and irregularly arranged collagen, whereas 810-nm light treatment showed compact and well-aligned collagen fibers. *Scale bar*, 50 μm (*bottom panels*)

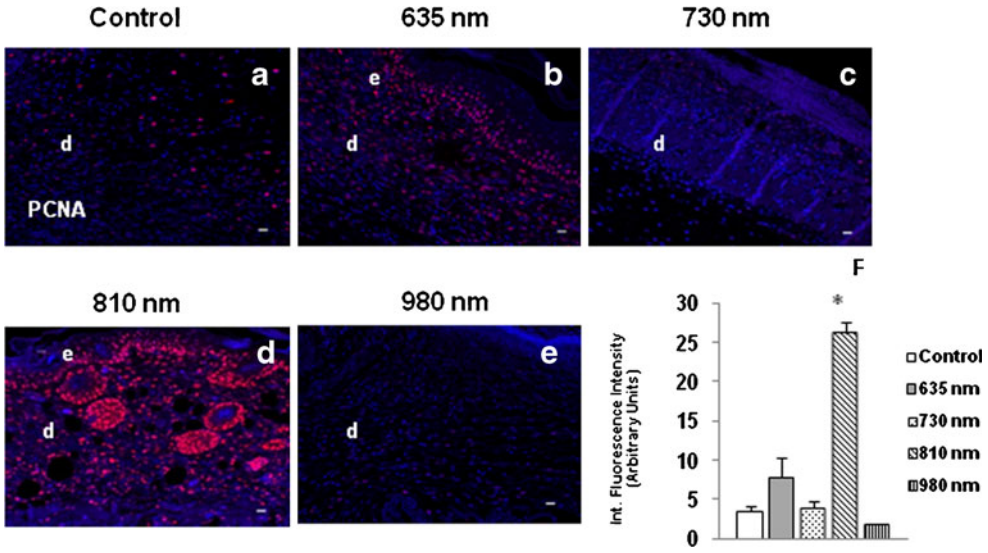

Fig. 3 Representative images of PCNA immunofluorescence staining on day 8 post-injury in partial-thickness dermal abrasion in mice showing enhanced cellular proliferation as evidenced by increased expression of PCNA in 810-nm light-treated wound compared with the non-illuminated control and other light (635, 730, and 980 nm) treated groups. **a**–**e** Immunofluorescence of PCNA and DAPI are represented by *red* and *blue* pseudo-colors, respectively. DAPI is used for nuclear counter stain. *Scale bar*, 20 μm (*bottom panels*). *d* dermis, *e* epidermis. **f** Integrated immunofluorescence intensity of PCNA was quantitatively analyzed from digital immunofluorescence images using Fiji (ImageJ) software. Data are expressed as the mean value of integrated immunofluorescence intensity of PCNA±SE ($n=6$ per group). *$p<0.05$ compared with the non-illuminated control and other light (635, 730, and 980 nm) treated groups

wound surface and dermal granulation tissue was evident in 810-nm treatment. The rapid wound healing in 810-nm-treated mice might be attributed to the photobiostimulative effects on the non-wounded healthy tissue, which in turn induces the unwounded keratinocytes and endothelial cells in the surrounding skin to migrate into the wounded area and promote re-epithelialization and angiogenesis. The fact that red and NIR lights can penetrate into deep tissue injury allows noninvasive treatment to be carried out for augmented healing processes. Visible red light (660 nm) is readily

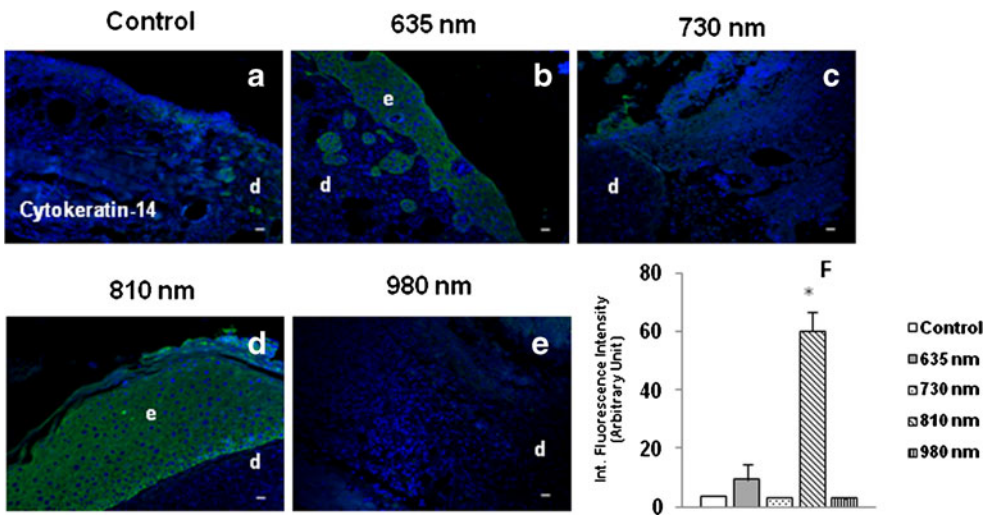

Fig. 4 Representative images of cytokeratin-14 immunofluorescence staining on day 8 post-injury in partial-thickness dermal abrasion in mice showing complete re-epithelialization as evidenced by enhanced expression of cytokeratin-14 in 810-nm light-treated wound compared with the non-illuminated control and other light (635, 730, and 980 nm) treated groups. **a**–**e** Immunofluorescence of cytokeratin-14 and DAPI are represented by *green* and *blue* pseudo-colors, respectively. DAPI is used for nuclear counter stain. *Scale bar*, 20 μm (*bottom panels*). *d* dermis, *e* epidermis. **f** Integrated immunofluorescence intensity of cytokeratin-14 was quantitatively analyzed from digital immunofluorescence images using Fiji (ImageJ) software. Data are expressed as the mean value of integrated immunofluorescence intensity of cytokeratin-14±SE ($n=6$ per group). *$p<0.05$ compared with the non-illuminated control and other light (635, 730, and 980 nm) treated groups

absorbed by blood and skin surface components, thereby limiting its tissue penetration to <10 mm. NIR laser 810 nm is not readily absorbed and has a much larger depth of tissue penetration of 30–40 mm or greater, thereby providing greater deposition of photons in the wound bed [11]. The effectiveness of 810-nm light agrees with previous publications which showed positive healing effects of 810 nm in in vitro and in vivo studies performed on cortical neurons, bone marrow-derived dendritic cells, and traumatic brain injury mouse models [7, 12]. These studies suggested that LLLT at 810-nm wavelength and lower fluence is capable of inducing mediators of cell signaling processes which in turn may be responsible for the beneficial stimulatory effects of LLLT; however, at higher fluencies, beneficial effects are reduced.

Light must be absorbed by a photoacceptor to exert photobiomodulation effects on living biological systems. Indeed, recent studies identified mitochondrial photoacceptor CCO as a principal tissue chromophore for visible/NIR spectral light [18, 23]. During LLLT, the absorption of red or NIR photons by CCO in the mitochondrial respiratory chain causes an increase in cellular respiration that leads to an increase in the production of ATP, which is required for numerous cellular functions, providing both energy and phosphates required for the regulation of cellular functions [20]. CCO has distinct absorption bands in the red (around 665 nm) and in the NIR (around 810 nm) regions [29]. There is minimum absorption of light by CCO at 730 nm, and there have been reports that this wavelength is ineffective in preserving cultured cortical neurons from cyanide toxicity [21] and also did not improve the neurobehavioral performance of mice after closed-head traumatic brain injury [12], while 665- to 670-nm and 810- to 830-nm wavelengths were highly active in the healing process [12, 29]. In the present study, the 980-nm wavelength was found ineffective. However, it should be mentioned that several reports show that 980 nm is an active wavelength in LLLT applications [30, 31]. It is entirely possible that our finding that 980 nm was ineffective only meant that we used suboptimal irradiation dosage parameters. In other words, if the fluence or fluence rate of the 980-nm laser was lower than we used (or possibly higher), the effect on dermal healing might have been positive.

In conclusion, the findings of the present study would suggest that photobiostimulation-induced healing for partial-thickness dermal abrasion in mice treated with red (635 nm) and NIR (810 nm) lights is attributed to modulating various phases of the wound healing process which include cellular proliferation, neovascularization, collagen accumulation, and re-epithelialization of the wound bed. However, healing was more pronounced in 810-nm as compared to 635-nm light treatment, which could be attributed to the greater penetration and to the absorption spectrum of cytochrome c oxidase, the candidate mitochondrial chromophore in LLLT.

Acknowledgments This work was funded by the US NIH (R01AI050875). Asheesh Gupta was supported by BOYSCAST Fellowship 2010-11 (Department of Science and Technology, Govt. of India). Tianhong Dai was supported by an Airlift Research Foundation Extremity Trauma Research Grant (grant 109421). We would like to acknowledge and deeply thank Jie Zhao, PhD, for her expertise and guidance with confocal microscopy and Peggy Sherwood and Julie LaGraves for their technical help with histology.

References

1. Zhang Y, Song S, Fong CC, Tsang CH, Yang Z, Yang M (2003) cDNA microarray analysis of gene expression profiles in human fibroblast cells irradiated with red light. J Invest Dermatol 120(5):849–857
2. Peplow PV, Chung TY, Ryan B, Baxter GD (2011) Laser photobiomodulation of gene expression and release of growth factors and cytokines from cells in culture: a review of human and animal studies. Photomed Laser Surg 29(5):285–304
3. Hawkins DH, Abrahamse H (2006) The role of laser fluence in cell viability, proliferation, and membrane integrity of wounded human skin fibroblasts following helium-neon laser irradiation. Lasers Surg Med 38(1):74–83
4. Chen CH, Hung HS, Hsu SH (2008) Low-energy laser irradiation increases endothelial cell proliferation, migration, and eNOS gene expression possibly via PI3K signal pathway. Lasers Surg Med 40(1):46–54
5. Fushimi T, Inui S, Nakajima T, Ogasawara M, Hosokawa K, Itami S (2012) Green light emitting diodes accelerate wound healing: characterization of the effect and its molecular basis in vitro and in vivo. Wound Repair Regen 20(2):226–235
6. Pereira AN, Eduardo Cde P, Matson E, Marques MM (2002) Effect of low-power laser irradiation on cell growth and procollagen synthesis of cultured fibroblasts. Lasers Surg Med 31(4):263–267
7. Sharma SK, Kharkwal GB, Sajo M, Huang YY, De Taboada L, McCarthy T, Hamblin MR (2011) Dose response effects of 810 nm laser light on mouse primary cortical neurons. Lasers Surg Med 43(8):851–859
8. Demidova-Rice TN, Salomatina EV, Yaroslavsky AN, Herman IM, Hamblin MR (2007) Low-level light stimulates excisional wound healing in mice. Lasers Surg Med 39(9):706–715
9. Meirelles GC, Santos JN, Chagas PO, Moura AP, Pinheiro AL (2008) A comparative study of the effects of laser photobiomodulation on the healing of third-degree burns: a histological study in rats. Photomed Laser Surg 26(2):159–166
10. Prabhu V, Rao SB, Chandra S, Kumar P, Rao L, Guddattu V, Satyamoorthy K, Mahato KK (2012) Spectroscopic and histological evaluation of wound healing progression following low level laser therapy (LLLT). J Biophotonics 5(2):168–184
11. Peplow PV, Chung TY, Baxter GD (2012) Laser photostimulation (660 nm) of wound healing in diabetic mice is not brought about by ameliorating diabetes. Lasers Surg Med 44(1):26–29
12. Wu Q, Xuan W, Ando T, Xu T, Huang L, Huang YY, Dai T, Dhital S, Sharma SK, Whalen MJ, Hamblin MR (2012) Low-level laser therapy for closed-head traumatic brain injury in mice: effect of different wavelengths. Lasers Surg Med 44(3):218–226
13. Christie A, Jamtvedt G, Dahm KT, Moe RH, Haavardsholm EA, Hagen KB (2007) Effectiveness of nonpharmacological and nonsurgical interventions for patients with rheumatoid arthritis: an overview of systematic reviews. Phys Ther 87(12):1697–1715
14. Naeser MA, Hahn KA, Lieberman BE, Branco KF (2002) Carpal tunnel syndrome pain treated with low-level laser and

microamperes transcutaneous electric nerve stimulation: a controlled study. Arch Phys Med Rehabil 83(7):978–988
15. Chow RT, Johnson MI, Lopes-Martins RA, Bjordal JM (2009) Efficacy of low-level laser therapy in the management of neck pain: a systematic review and meta-analysis of randomised placebo or active-treatment controlled trials. Lancet 374(9705):1897–1908
16. Flemming KA, Cullum NA, Nelson EA (1999) A systematic review of laser therapy for venous leg ulcers. J Wound Care 8(3):111–114
17. Chung H, Dai T, Sharma SK, Huang YY, Carroll JD, Hamblin MR (2012) The nuts and bolts of low-level laser (light) therapy. Ann Biomed Eng 40(2):516–533
18. Karu TI, Kolyakov SF (2005) Exact action spectra for cellular responses relevant to phototherapy. Photomed Laser Surg 23(4):355–361
19. Oron U (2011) Light therapy and stem cells: a therapeutic intervention of the future? Interv Cardiol 3(6):627–629
20. Lane N (2006) Cell biology: power games. Nature 443(7114):901–903
21. Wong-Riley MT, Liang HL, Eells JT, Chance B, Henry MM, Buchmann E, Kane M, Whelan HT (2005) Photobiomodulation directly benefits primary neurons functionally inactivated by toxins: role of cytochrome c oxidase. J Biol Chem 280(6):4761–4771
22. Pastore D, Greco M, Petragallo VA, Passarella S (1994) Increase in $\leftarrow H^+/e^-$ ratio of the cytochrome c oxidase reaction in mitochondria irradiated with helium–neon laser. Biochem Mol Biol Int 34(4):817–826
23. Karu T (1999) Primary and secondary mechanisms of action of visible to near-IR radiation on cells. J Photochem Photobiol B 49(1):1–17
24. Posten W, Wrone DA, Dover JS, Arndt KA, Silapunt S, Alam M (2005) Low-level laser therapy for wound healing: mechanism and efficacy. Dermatol Surg 31(3):334–340
25. Basford JR (1995) Low intensity laser therapy: still not an established clinical tool. Lasers Surg Med 16(4):331–342
26. Pontinen PJ, Aaltokallio T, Kolari PJ (1996) Comparative effects of exposure to different light sources (He–Ne laser, InGaAl diode laser, a specific type of noncoherent LED) on skin blood flow for the head. Acupunct Electrother Res 21(2):105–118
27. Bisht D, Gupta SC, Misra V, Mital VP, Sharma P (1994) Effect of low intensity laser radiation on healing of open skin wounds in rats. Indian J Med Res 100:43–46
28. Fahimipour F, Mahdian M, Houshmand B, Asnaashari M, Sadrabadi AN, Farashah SE, Mousavifard SM, Khojasteh A (2013) The effect of He–Ne and Ga–Al–As laser light on the healing of hard palate mucosa of mice. Lasers Med Sci 28:93–100
29. Karu TI, Pyatibrat LV, Kolyakov SF, Afanasyeva NI (2005) Absorption measurements of a cell monolayer relevant to phototherapy: reduction of cytochrome c oxidase under near IR radiation. J Photochem Photobiol B 81(2):98–106
30. Park JJ, Kang KL (2012) Effect of 980-nm GaAlAs diode laser irradiation on healing of extraction sockets in streptozotocin-induced diabetic rats: a pilot study. Lasers Med Sci 27(1):223–230
31. Skopin MD, Molitor SC (2009) Effects of near-infrared laser exposure in a cellular model of wound healing. Photodermatol Photoimmunol Photomed 25(2):75–80